IEEE Access
Multidisciplinary ⋮ Rapid Review ⋮ Open Access Journal

Received 1 August 2022, accepted 19 September 2022, date of publication 21 September 2022, date of current version 28 September 2022.

Digital Object Identifier 10.1109/ACCESS.2022.3208412

RESEARCH ARTICLE

Robust Adaptive Super-Twisting Sliding Mode Stability Control of Underactuated Rotational Inverted Pendulum With Experimental Validation

FAYEZ F. M. EL-SOUSY[1], (Member, IEEE), KHALID A. ALATTAS[2], (Member, IEEE), OMID MOFID[3], SALEH MOBAYEN[3], (Senior Member, IEEE), AND AFEF FEKIH[4], (Senior Member, IEEE)

[1]Department of Electrical Engineering, College of Engineering, Prince Sattam Bin Abdulaziz University, Al-Kharj 16278, Saudi Arabia
[2]Department of Computer Science and Artificial Intelligence, College of Computer Science and Engineering, University of Jeddah, Jeddah 23218, Saudi Arabia
[3]Future Technology Research Center, National Yunlin University of Science and Technology, Douliou, Yunlin 64002, Taiwan
[4]Department of Electrical and Computer Engineering, University of Louisiana at Lafayette, Lafayette, LA 70504, USA

Corresponding author: Saleh Mobayen (mobayens@yuntech.edu.tw)

This work was supported in part by the National Science and Technology Council (NSTC), Taiwan, under Grant NSTC 110-2221-E-224-050-.

ABSTRACT In this study, an adaptive proportional-integral-derivative (PID) sliding mode control technique combined with the super-twisting algorithm is planned for the stabilization of rotational inverted pendulum in the appearance of exterior perturbation. The state-space model of rotational inverted pendulum in the existence of exterior disturbance is attained. Then, the super-twisting PID sliding mode controller is designed for finite time stability control of the considered underactuated control system. The upper bounds of perturbation are presumed to be unknown; consequently, the adaptive control procedure is taken into account to approximate the uncertain bounds of external disturbances. The stability control of rotational inverted pendulum system is verified by means of the Lyapunov stability theory. In order to validate the accuracy and efficiency of the recommended control technique, some simulation outcomes are prepared and compared with other existing scheme. Finally, the experimental results are implemented to show the success of the designed method.

INDEX TERMS Robust control, adaptive tuning, underactuated systems, sliding mode control, inverted pendulum.

I. INTRODUCTION

Rotary (rotational) inverted pendulum (RIP) system is considered as an underactuated system which has been established by Furuta with the help of his college at first [1], [2], [3], [4], [5], [6]. This system contains a rotational arm and a pendulum linked at the end of the arm. The arm can move in the horizontal plane as well as pendulum has movement in the vertical plane [7], [8], [9], [10], [11], [12], [13]. Various types of physical systems such as human's arm motion, control of position and attitude of aircrafts, and robot system have been originated from the model of RIP system [14], [15], [16]. For this reason, stability and control of RIP system is still in consideration [17], [18], [19], [20]. Hence, the control problem of RIP system is divided into two subsystems. In the first subsystem, the stability of position and angular velocity relevant to the arm of RIP system is investigated. In addition, in the second subsystem, the main goal of control is the balancing of pendulum to be stand up-right [21], [22], [23], [24]. Therefore, some control methods including proportional-integral-derivative (PID), linear quadratic regulator (LQR), linear quadratic Gaussian (LQG), linear matrix inequality (LMI) [25], sliding mode control (SMC), adaptive-control, fuzzy logic and neural network [26] techniques have been applied for both stability and balancing control of RIP systems [18], [27], [28], [29], [30], [31].

In [32], LOR and LQG methods based on the fuzzy logic controltechnique has been proposed aimed at stability control of double-RIP system under perturbation. Besides, these methods are compared with the classical LOR and LQG

The associate editor coordinating the review of this manuscript and approving it for publication was Jason Gu.

techniques which confirm better performance of the proposed methods. In [33], an LQR control scheme decoupled PID control technique is designed in order to stability and balancing control of RIP systems. In [34], a robust LQR controller is presented based on the adaptive fuzzy logic control technique mixed with neural network in the target of stability and balancing control of RIP system. In [35], an observer for inverted pendulum system is designed based on the adaptive technique using auxiliary variable. On the other hand, an auxiliary observer is used for approximation of the external disturbance and an adaptive observer is applied for estimation of states and uncertain parameters. In [36], an adaptive integral SMC technique is designed for the wheeled inverted pendulum system in the presence of external disturbance and parametric uncertainty. In addition, this method forces that the state of the system is converged to the origin in the finite time. In [37], the dynamic model of double inverted pendulum combined with crane system is presented. Then, an adaptive SMC (ASMC) scheme is proposed for stabilization and tracking control of derived system by using Lyapunov and LaSalle's theory [38], [39], [40], [41]. In [42], three methods, i.e., second-order SMC, proportional-derivative SMC and ASMC are designed for Furuta inverted pendulum system. To the best of the authors' knowledge, no robust adaptive super-twisting sliding mode stability control method has been investigated for the underactuated rotary inverted pendulum systems in the presence of external disturbances.

According to the above-mentioned discussion about the stability control of RIP system, it can be inferred that rare researches have paid attention to the finite-time stabilization control of underactuated RIP system in the presence of external disturbance using adaptive supper-twisting PID-SMC method. In this paper, firstly, a PID-SMC-based super-twisting method is used for finite-time stabilization control of RIP system in the existence of known bounded disturbances. Whereas upper bound of perturbation is unknow, PID-ASMC mixed super-twisting technique is planned for the estimation if the upper bound of disturbance which is entered to the RIP system. Thus, the key novelties of this paper can be listed as follows:

- Design of PID-SMC combined super-twisting algorithm for finite-time stability control of RIP system under known bounded perturbation;
- Proposing of PID-ASMC for stability control of RIP system with unknown bounded external disturbance;
- Finite-time reachability of the proposed PID-switching surface by means of Lyapunov theory concept.

The rest of this paper is formed as follows: in Sect. II, model description of the RIP system is expressed. The state-space form of RIP system in the existence of disturbance is obtained in Sect. III. In Sect. IV, PID-ASMC strategy based on super-twisting method is presented. Simulation outcomes are provided in Sect. V. The fundamental conclusion of the paper is reported in Sect. VI.

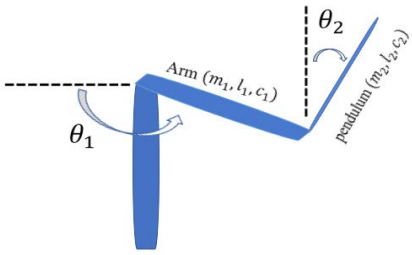

FIGURE 1. Rotational inverted pendulum configuration.

II. MATHEMATICAL MODEL DESCRIPTION

The schematic configuration of rotary inverted pendulum system is depicted in Fig.1. Consider $\boldsymbol{\theta_1}$ and $\boldsymbol{\theta_2}$ are the angular displacement of arm and angular displacement of pendulum, respectively. The terms $\boldsymbol{m_1}$, $\boldsymbol{l_1}$ and $\boldsymbol{c_1}$ are the mass, length and distance to the center of arm. Also, $\boldsymbol{m_2}$, $\boldsymbol{l_2}$ and $\boldsymbol{c_2}$ denote the mass, length and distance to pendulum's center, correspondingly.

Dynamic equation of rotational inverted pendulum is expressed as

$$M(\theta)\ddot{\theta} + V\left(\theta, \dot{\theta}\right)\dot{\theta} + G(\theta) = \tau \tag{1}$$

where $\theta = [\theta_1, \theta_2]^T$. The terms M, V, G and τ are the mass, Coriolis and Centripetal, gravitational and torque matrixes, respectively, which are given as follow:

$$M = \begin{bmatrix} J_1 + m_2 l_2 + m_2 c_2^2 sin^2(\theta_2) & m_2 l_1 c_2 cos(\theta_2) \\ m_2 l_1 c_2 cos(\theta_2) & J_2 + m_2 c_2^2 \end{bmatrix}, \tag{2}$$

$$V = \frac{1}{2} m_2 \begin{bmatrix} l_1^2 \dot{\theta}_2 s_{2\theta_2} & -2 l_1 c_2 \dot{\theta}_2 s_{\theta_2} + c_2^2 \dot{\theta}_1 s_{2\theta_2} \\ -c_2 \dot{\theta}_1 c_{2\theta_2} & 0 \end{bmatrix} \tag{3}$$

$$G = \begin{bmatrix} 0 \\ -m_2 c_2 g \sin(\theta_2) \end{bmatrix}, \tag{4}$$

$$\tau = \begin{bmatrix} \tau_1 \\ 0 \end{bmatrix}. \tag{5}$$

where J_1, J_2, g and τ_1 are the moment of the arm's inertia, moment of the pendulum's inertia, gravitational acceleration and applied torque, respectively. Moreover, we define $s_{2\theta_2} = \sin(2\theta_2)$, $c_{2\theta_2} = c(2\theta_2)$ and $s_{\theta_2} = \sin(\theta_2)$.

Consider that Eq. (1) is rewritten as follow:

$$\ddot{\theta} + M^{-1}(\theta) V\left(\theta, \dot{\theta}\right)\dot{\theta} + M^{-1}(\theta) G(\theta) = M^{-1}(\theta)\tau, \tag{6}$$

where M^{-1} is the inversion of matrix M. After simplification and substituting Eqs. (4),(5) into Eq. (6), one can obtain

$$\begin{aligned} \begin{bmatrix} \ddot{\theta}_1 \\ \ddot{\theta}_2 \end{bmatrix} = &- \begin{bmatrix} M_{11} & M_{12} \\ M_{21} & M_{22} \end{bmatrix} \begin{bmatrix} v_{11} & v_{12} \\ v_{21} & v_{22} \end{bmatrix} \begin{bmatrix} \dot{\theta}_1 \\ \dot{\theta}_2 \end{bmatrix} \\ &- \begin{bmatrix} M_{11} & M_{12} \\ M_{21} & M_{22} \end{bmatrix} \begin{bmatrix} 0 \\ -m_2 c_2 g \sin(\theta_2) \end{bmatrix} \\ &+ \begin{bmatrix} M_{11} & M_{12} \\ M_{21} & M_{22} \end{bmatrix} \begin{bmatrix} \tau_1 \\ 0 \end{bmatrix}, \end{aligned} \tag{7}$$

where M_{11}, M_{12}, M_{21} and M_{22} are the elements of matrix M^{-1} and v_{11}, v_{12}, v_{21} and v_{22} denote the components of the

matrix V. Now, by multiplying the matrices and doing some simplifications, we have

$$\begin{bmatrix}\ddot{\theta}_1\\ \ddot{\theta}_2\end{bmatrix} = \begin{bmatrix}-M_{11}v_{11}-M_{12}v_{21} & -M_{11}v_{12}-M_{12}v_{22}\\ -M_{21}v_{11}-M_{22}v_{21} & -M_{21}v_{12}-M_{22}v_{22}\end{bmatrix}\begin{bmatrix}\dot{\theta}_1\\ \dot{\theta}_2\end{bmatrix} + \begin{bmatrix}M_{12}m_2c_2gs_{\theta_2}\\ M_{22}m_2c_2gs_{\theta_2}\end{bmatrix} + \begin{bmatrix}M_{11}\tau_1\\ M_{21}\tau_1\end{bmatrix}. \quad (8)$$

Define $F_1 = -M_{11}v_{11} - M_{12}v_{21}$, $F_2 = -M_{11}v_{12} - M_{12}v_{22}$, $F_3 = M_{12}m_2c_2gs_{\theta_2}$, $F_4 = -M_{21}v_{11} - M_{22}v_{21}$, $F_5 = -M_{21}v_{12} - M_{22}v_{22}$ and $F_6 = M_{22}m_2c_2gs_{\theta_2}$; so, the dynamical equation of rotary inverted pendulum is written as

$$\ddot{\theta}_1 = F_1\dot{\theta}_1 + F_2\dot{\theta}_2 + F_3 + M_{11}\tau_1, \quad (9)$$
$$\ddot{\theta}_2 = F_4\dot{\theta}_1 + F_5\dot{\theta}_2 + F_6 + M_{21}\tau_1. \quad (10)$$

III. PROBLEM DESCRIPTION AND ASSUMPTIONS

In this part, the dynamical model of rotary inverted pendulum system is offered in the state-space form in the appearance of external disturbances. Afterward, the required assumption is studied.

Consider $Y = [y_1, y_2, y_3, y_4]^T = \left[\theta_1, \dot{\theta}_1, \theta_2, \dot{\theta}_2\right]^T$ and $\Delta = [\Lambda_1, \Lambda_2]^T$ as the state-space variable and external disturbance vectors, respectively. The dynamic model (9)-III is expressed in the state-space form with external disturbances as

$$\dot{y}_1(t) = y_2(t), \quad (11)$$
$$\dot{y}_2(t) = F_1y_2(t) + F_2y_4(t) + F_3 + M_{11}\tau_1(t) + \Lambda_1(t), \quad (12)$$
$$\dot{y}_3(t) = y_4(t), \quad (13)$$
$$\dot{y}_4(t) = F_4y_2(t) + F_5y_4(t) + F_6 + M_{21}\tau_1(t) + \Lambda_2(t). \quad (14)$$

Assumption 1: Presume that the constrained exterior perturbations Λ_1, Λ_2 fulfill the subsequent conditions:

$$|w_3\Lambda_1(t)| \le \beta_1, \quad (15)$$
$$|w_4\Lambda_2(t)| \le \beta_2, \quad (16)$$

where β_1 and β_2 are the unknown positive constants, and w_i's are positive constants.

IV. ADAPTIVE SUPER-TWISTING PID SLIDING MODE CONTROL

In this part, the stability control of rotational inverted pendulum is investigated using super-twisting PID sliding mode control technique. For this reason, the PID sliding surface is defined as

$$s(t) = w_1y_1(t) + w_2y_3(t) + w_3y_2(t) + w_4y_4(t) + \kappa_I\int_0^t (y_1(\Upsilon) + y_3(\Upsilon))d\Upsilon, \quad (17)$$

where κ_I is the positive constant. Taking time-derivative of (17), it yields

$$\dot{s}(t) = w_1\dot{y}_1(t) + w_2\dot{y}_3(t) + w_3\dot{y}_2(t) + w_4\dot{y}_4(t) + \kappa_I(y_1(t) + y_3(t)). \quad (18)$$

Substituting Eqs. (11)-IV into (18), we have

$$\dot{s}(t) = w_1(y_2(t)) + w_2(y_4(t)) + w_3(F_1y_2(t) + F_2y_4(t) + F_3 + M_{11}\tau_1(t) + \Lambda_1(t) + w_4(F_4y_2(t) + F_5y_4(t) + F_6 + M_{21}\tau_1(t) + \Lambda_2(t)) + \kappa_I(y_1(t) + y_3(t)). \quad (19)$$

After some simplification, we can get

$$\dot{s}(t) = (w_1 + w_3F_1 + w_4F_4)y_2(t) + (w_2 + w_3F_2 + w_4F_5)y_4(t) + (w_3F_3 + w_4F_6) + \kappa_I(y_1(t) + y_3(t)) + (w_3M_{11} + w_4M_{21})\tau_1(t) + w_3\Lambda_1(t) + w_4\Lambda_2(t). \quad (20)$$

Now, the super-twisting PID sliding mode controller is defined as

$$\tau_1(t) = -\frac{1}{w_3M_{11} + w_4M_{21}}(\tau_{1_{eq}} + \tau_{1_{st}}), \quad (21)$$

where

$$\tau_{1_{eq}} = (w_1 + w_3F_1 + w_4F_4)y_2(t) + (w_2 + w_3F_2 + w_4F_5)y_4(t) + (w_3F_3 + w_4F_6) + \kappa_I(y_1(t) + y_3(t) + \beta_1 sign(s(t)) + \beta_2 sign(s(t))), \quad (22)$$
$$\tau_{1_{st}} = \sigma_1\sqrt{s(t)}sign(s(t)) + \sigma_2 sign(s(t)) \quad (23)$$

with σ_1 and σ_2 as the positive constants.

The objective of the following theorem is the finite time stability of the rotational inverted pendulum in the existence of external disturbance with known bounds.

Theorem 1: Assume that the dynamical equation of rotational inverted pendulum be as (11)-IV and the PID sliding surface and control input are designed as (17) and (21). Then, the finite-time convergence of the planned sliding surface to the origin is proved and the system's stability control is performed.

Proof: Consider the candidate Lyapunov function as

$$V(t) = 0.5s(t)^2. \quad (24)$$

Taking derivative of (24) with respect to time and using (20), it can obtain

$$\dot{V}(t) = s(t)\left[(w_1 + w_3F_1 + w_4F_4)y_2(t) + (w_2 + w_3F_2 + w_4F_5)y_4(t) + (w_3F_3 + w_4F_6) + \kappa_I(y_1(t) + y_3(t)) + (w_3M_{11} + w_4M_{21})\tau_1(t) + (w_3\Lambda_2(t) + w_4\Lambda_4(t))\right], \quad (25)$$

where substituting the control laws (21)-(23) into (25), one achieves

$$\begin{aligned}\dot{V}(t) = s(t)[&-\sigma_1\sqrt{s}sign(s) - \sigma_2 sign(s)\\ &-\beta_1 sign(s) - \beta_2 sign(s)\\ &+w_3\Lambda_1(t) + w_4\Lambda_2(t)].\end{aligned} \tag{26}$$

After some simplification, we have

$$\begin{aligned}\dot{V}(t) = &-\sigma_1\sqrt{s}|s| - \sigma_2|s| - \beta_1|s|\\ &-\beta_2|s(t)| + (w_3\Lambda_1(t) + w_4\Lambda_2(t))s(t).\end{aligned} \tag{27}$$

Considering Assumption 1 and doing some mathematical operations, it yields

$$\begin{aligned}\dot{V}(t) \le &-\sigma_1|s|^{\frac{3}{2}} - \sigma_2|s| - \beta_1|s| - \beta_2|s|\\ &+\beta_1|s(t)| + \beta_2|s(t)|,\end{aligned} \tag{28}$$

whereas $\sigma_1|s(t)|^{\frac{3}{2}}$ is a positive expression; so, it can be removed, therefore we have

$$\dot{V}(t) \le -\sigma_2|s(t)|, \tag{29}$$

where considering the Lyapunov function (24), we obtain

$$\dot{V}(t) \le -\sqrt{2}\sigma_2 V^{\frac{1}{2}}(t). \tag{30}$$

Hence, according to the above equation, the PID sliding surface is converged to zero in the finite time via the super-twisting controller. □

Remark 1: The adaptive control technique is an effective method for aproximatation of the upper bounds of exterior perturbation which is unknown in practical and actual applications. Thus, in the following theorem, an adaptive-tunning scheme is applied to estimate the upper bound of exterior disturbance. For thispurpose, the estimation errors are defined as

$$\tilde{\beta}_1(t) = \beta_1 - \hat{\beta}_1(t), \tag{31}$$
$$\tilde{\beta}_2(t) = \beta_2 - \hat{\beta}_2(t), \tag{32}$$

where $\hat{\beta}_1(t)$ and $\hat{\beta}_2(t)$ are the estimated values of β_1 and β_2. The adaptive laws can be offered as

$$\dot{\hat{\beta}}_1(t) = a_1^{-1}(|s(t)| - b_{m1}^2\hat{\beta}_1(t)), \tag{33}$$
$$\dot{\hat{\beta}}_2(t) = a_2^{-1}(|s(t)| - b_{m2}^2\hat{\beta}_2(t)), \tag{34}$$

where a_1 and a_2 are the positive constants and b_{m1} and b_{m2} are achieved by the following equations:

$$\dot{b}_{m1} = -k_{m1}b_{m1}, \tag{35}$$
$$\dot{b}_{m2} = -k_{m2}b_{m2}, \tag{36}$$

while k_{m1} and k_{m2} signify the positive constants. Thus, the control input is designed as

$$\tau_1(t) = -\frac{1}{w_3M_{11}+w_4M_{21}}(\tau_{1_{eq}} + \tau_{1_{st}}), \tag{37}$$

where

$$\begin{aligned}\tau_{1_{eq}} = &(w_1 + w_3F_1 + w_4F_4)y_2(t)\\ &+(w_2 + w_3F_2 + w_4F_5)y_4(t) + (w_3F_3 + w_4F_6)\\ &+\kappa_I(y_1(t) + y_3(t) + \hat{\beta}_1 sign(s(t))\\ &+\hat{\beta}_2 sign(s(t))),\end{aligned} \tag{38}$$

$$\tau_{1_{st}} = \sigma_1\sqrt{s(t)}sign(s(t)) + \sigma_2 sign(s(t)). \tag{39}$$

Theorem 2: For the rotary inverted pendulum system (11)-IV under known external disturbance which holds Assumption 1, the control inputs (37)-(39) are designed based on the sliding surface (17) and adaptive laws (33)-(36). Thus, the sliding surface is converged to the origin as well as the stability control of the underactuated system is fulfilled.

Proof: Form the candidate Lyapunov function as follow:

$$\begin{aligned}V(t) = &0.5s(t)^2 + 0.5a_1\tilde{\beta}_1^2(t) + 0.5a_2\tilde{\beta}_2^2(t)\\ &+\frac{1}{8}k_{m1}^{-1}(\beta_1 b_{m1})^2 + \frac{1}{8}k_{m2}^{-1}(\beta_2 b_{m2})^2,\end{aligned} \tag{40}$$

where respect to the time-derivative of Eq. (40) and considering $\dot{\tilde{\beta}}_1(t) = -\dot{\hat{\beta}}_1(t)$ and $\dot{\tilde{\beta}}_2(t) = -\dot{\hat{\beta}}_2(t)$, it obtains

$$\begin{aligned}\dot{V}(t) = &s\dot{s} + a_1\tilde{\beta}_1(t)\dot{\hat{\beta}}_1(t) + a_2\tilde{\beta}_2(t)\dot{\hat{\beta}}_2(t)\\ &+\frac{1}{4}k_{m1}^{-1}\beta_1\dot{b}_{m1}(\beta_1 b_{m1}) + \frac{1}{4}k_{m2}^{-1}\beta_2\dot{b}_{m2}(\beta_2 b_{m2}).\end{aligned} \tag{41}$$

Now, the equations (20) and (33)-(36) are substituted into (41), then the subsequent equation is achieved

$$\begin{aligned}\dot{V}(t) = &s(t)[(w_1 + w_3F_1 + w_4F_4)y_2(t)\\ &+(w_2 + w_3F_2 + w_4F_5)y_4(t) + (w_3F_3 + w_4F_6)\\ &+\kappa_I(y_1(t) + y_3(t)) + (w_3M_{11} + w_4M_{21})\tau_1(t)\\ &+w_3\Lambda_1(t) + w_4\Lambda_2(t)] + \tilde{\beta}_1(t)\left(|s(t)| - b_{m1}^2\hat{\beta}_1(t)\right)\\ &+\tilde{\beta}_2(t)\left(|s(t)| - b_{m2}^2\hat{\beta}_2(t)\right) - \frac{1}{4}(\beta_1 b_{m1})^2\\ &-\frac{1}{4}(\beta_2 b_{m2})^2.\end{aligned} \tag{42}$$

Using the control laws (37)-(39), it gets

$$\begin{aligned}\dot{V}(t) = &s(t)\left[w_3\Lambda_1(t) + w_4\Lambda_2(t) - \sigma_1\sqrt{s}sign(s)\right.\\ &\left.-\sigma_2 sign(s) - \hat{\beta}_1(t)sign(s) - \hat{\beta}_2(t)sign(s)\right]\\ &+\tilde{\beta}_1(t)\left(|s(t)| - b_{m1}^2\hat{\beta}_1(t)\right)\\ &+\tilde{\beta}_2(t)\left(|s(t)| - b_{m2}^2\hat{\beta}_2(t)\right) - \frac{1}{4}(\beta_1 b_{m1})^2\\ &-\frac{1}{4}(\beta_2 b_{m2})^2.\end{aligned} \tag{43}$$

According to Assumption 1, we have

$$\begin{aligned}\dot{V}(t) \le &-\sigma_1|s|^{\frac{3}{2}} - \sigma_2|s| + (\beta_1 - \hat{\beta}_1(t))|s|\\ &+(\beta_2 - \hat{\beta}_2(t))|s| - \tilde{\beta}_1(t)|s| - \tilde{\beta}_2(t)|s|\\ &+b_{m1}^2\tilde{\beta}_1(t)\hat{\beta}_1(t) + b_{m2}^2\tilde{\beta}_2(t)\hat{\beta}_2(t) - \frac{1}{4}(\beta_1 b_{m1})^2\\ &-\frac{1}{4}(\beta_2 b_{m2})^2.\end{aligned} \tag{44}$$

TABLE 1. Rotary-inverted- pendulum parameters.

Parameter	Value	Parameter	Value
$m_1(kg)$	0.056	m_2(kg)	0.022
$l_1(m)$	0.16	l_2(m)	0.16
$c_1(m)$	0.08	$c_2(m)$	0.08
$J_1(Nm/rads)$	0.001569	$J_2\ (Nm/rads)$	0.0001785

From Eqs. (31) and (32) and removing the similar terms, we can obtain

$$\dot{V}(t) \leq -\sigma_1 |s(t)|^{\frac{3}{2}} - \sigma_2 |s(t)| + b_{m1}^2(\beta_1 - \hat{\beta}_1(t))\hat{\beta}_1(t) + b_{m2}^2(\beta_2 - \hat{\beta}_2(t))\hat{\beta}_2(t) - \frac{1}{4}(\beta_1 b_{m1})^2 - \frac{1}{4}(\beta_2 b_{m2})^2, \quad (45)$$

where by simplification, it yields

$$\dot{V}(t) \leq -\sigma_1 |s|^{\frac{3}{2}} - \sigma_2 |s| + b_{m1}^2\beta_1\hat{\beta}_1(t) + b_{m2}^2\beta_2\hat{\beta}_2(t) - b_{m1}^2\hat{\beta}_1^2(t) - b_{m2}^2\hat{\beta}_2^2(t) - \frac{1}{4}(\beta_1 b_{m1})^2 - \frac{1}{4}(\beta_2 b_{m2})^2. \quad (46)$$

Now, consider the following inequalities [43]:

$$(\beta_1 b_{m1})(\hat{\beta}_1(t)\, b_{m1}) \leq \frac{1}{4}(\beta_1 b_{m1})^2 + b_{m1}^2\hat{\beta}_1^2(t), \quad (47)$$

$$(\beta_2 b_{m2})(\hat{\beta}_2(t)\, b_{m2}) \leq \frac{1}{4}(\beta_2 b_{m2})^2 + b_{m2}^2\hat{\beta}_2^2(t). \quad (48)$$

Substituting (47) and V into (46), the following equation is resulted:

$$\dot{V}(t) \leq -\sigma_1 |s(t)|^{\frac{3}{2}} - \sigma_2 |s(t)| + \frac{1}{4}(\beta_1 b_{m1})^2 + b_{m1}^2\hat{\beta}_1^2(t) + \frac{1}{4}(\beta_2 b_{m2})^2 + b_{m2}^2\hat{\beta}_2^2(t) - b_{m1}^2\hat{\beta}_1^2(t) - b_{m2}^2\hat{\beta}_2^2(t) - \frac{1}{4}(\beta_1 b_{m1})^2 - \frac{1}{4}(\beta_2 b_{m2})^2, \quad (49)$$

where by removing the same expressions, it leads to

$$\dot{V}(t) \leq -\sigma_1 |s|^{\frac{3}{2}} - \sigma_2 |s| \leq -\sigma_2 |s|. \quad (50)$$

Hence, we obtain $\dot{V}(t) \leq 0$. Therefore, it is demonstrated that the proposed switching surface converges to origin. The proof is finished. □

V. SIMULATION AND EXPERIMENTAL RESULTS

A. SIMULATION RESULTS

In this part, the simulation results for RIP system are performed based on the adaptive super-twisting PID-SMC technique as exposed in Fig.1. The constant parameters of RIP system and the design values are given in Table 1 and Table 2, correspondingly.

The simulation outcomes based on the planned scheme are compred with the method of [1] in two parts. The proosed PD sliding surface in [1] is defined as $s(t) = w_1 y_1(t) + w_2 y_3(t) + w_3 y_2(t) + w_4 y_4(t)$. At first, simulation results are obtained with the known upper bound of exterior disturbances. The finite time stablity of rotational inverted pendulum applying the super-twisting PID-SMC law is observed in Fig.3 and Fig.4. In Fig.3, the angular position and velocity of arm of

TABLE 2. Initial conditions and design parameters.

$\Lambda_1(t) = \Lambda_3(t) = 0.01\,sin(t)$	$\Lambda_2(t) = \Lambda_4(t) = 0.01\,cos(t)$
$w_1 = 10, w_3 = 5$	$w_2 = 20, w_4 = 10$
$a_1 = a_2 = 0.5$	$k_{m1} = k_{m2} = 0.5$
$\sigma_1 = 1.5, \sigma_2 = 0.01$	$[b_{m1}(0), b_{m2}(0)] = [0,0]$
$[\theta_1(0), \dot{\theta}_1(0), \theta_2(0), \dot{\theta}_2(0)] = \left[\frac{pi}{3,0}, -pi/15,0\right]$	$[\hat{\beta}_1(0), \hat{\beta}_2(0)] = [0.5,0.5]$

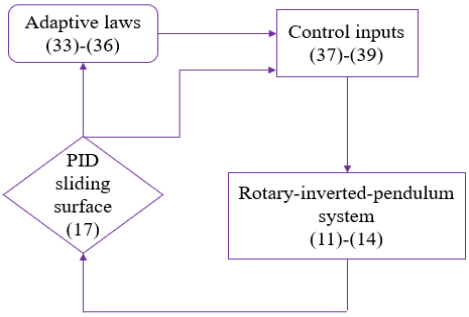

FIGURE 2. Block diagram of adaptive super-twisting PID-SMC scheme.

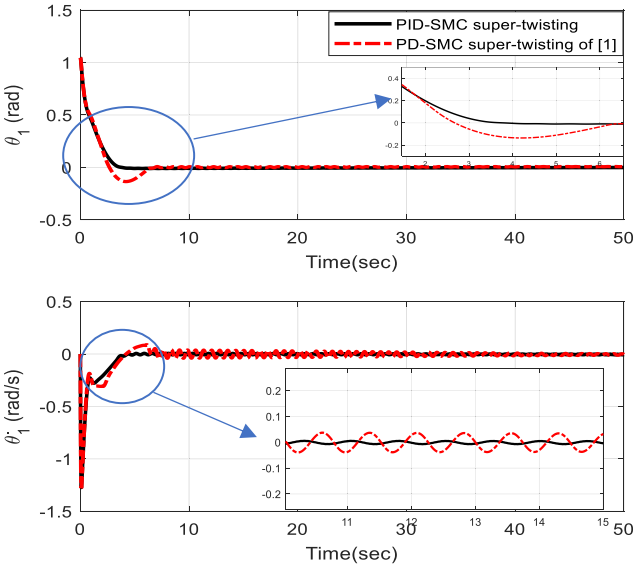

FIGURE 3. Time responses of angular position and velocity of arm of rotary inverted pendulum.

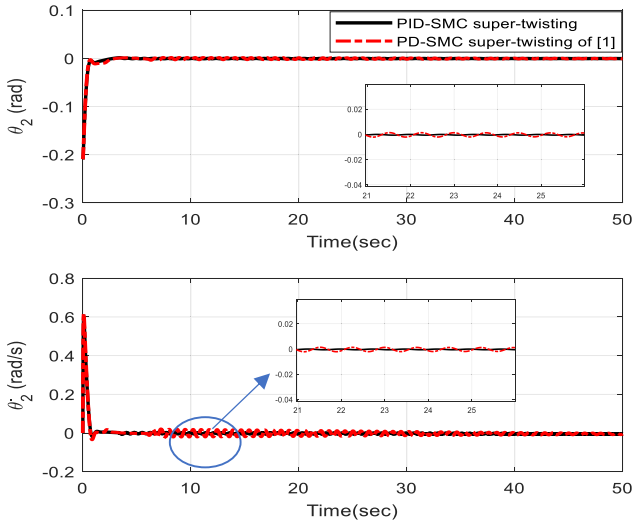

FIGURE 4. Time responses of angular position and velocity of inverted pendulum.

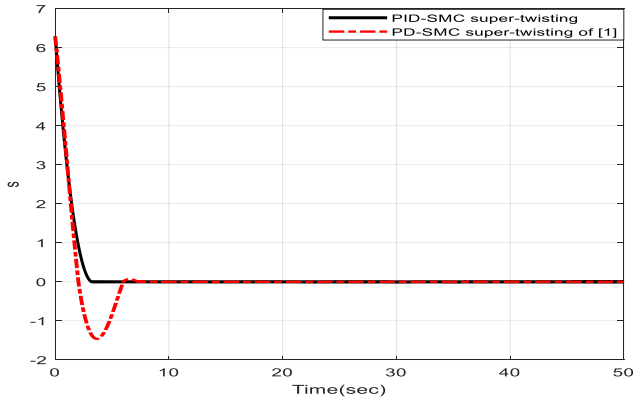

FIGURE 5. Time histories of sliding surface under known bound perturbation.

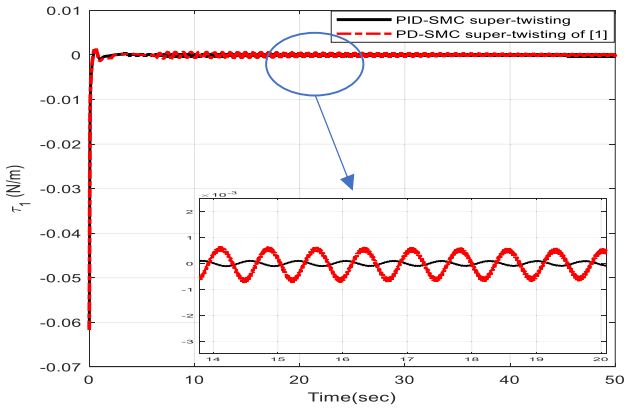

FIGURE 6. Time response of applied torque to rotary inverted pendulum system using super-twisting PID-SMC.

RIP system are illustrated. Fig.4 shows the time trajectories of angular position and angular velocity. Time histories of the sliding surfaces under known bound perturbation are

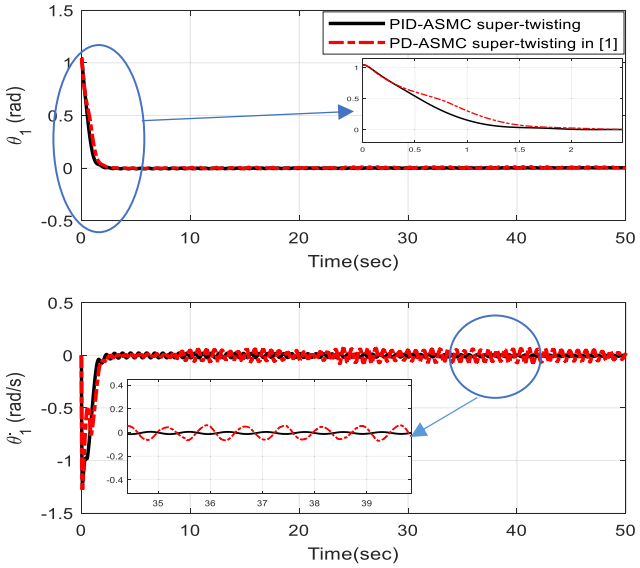

FIGURE 7. Time trajectories of angular position and velocity of arm of rotary-inverted-pendulum.

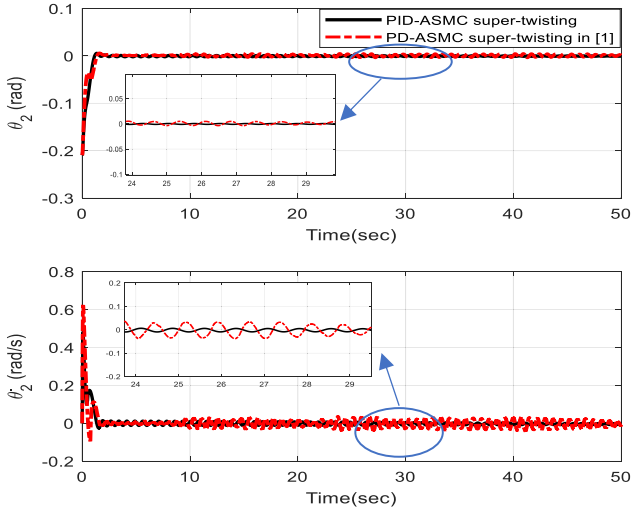

FIGURE 8. Time trajectories of angular position and velocity of inverted pendulum using adaptive supper-twisting PID-SMC.

presented in Fig. 5. The applied torque of the system which is gained by the super-twisting PID-SMC is shown in Fig.6. From these figures, it can be seen that not only the suggested method has quick response respect to the method of [1], but also the transient performnace of the recomende method is much better than method of [1].

Now, it is persumed that the upper bound of exterior disturbance is unknown. So, the simulation results are reimplemented using the adaptive control technique. The stability control of RIP system based on the adaptive super-twisitng PID sliding mode controller is exposed in Fig.7 and Fig.8. Also, time trajectory of reachability of sliding surface to origin is represented in Fig.9. Time response of the applied torque based on the adaptive super-twisting PID-SMC is

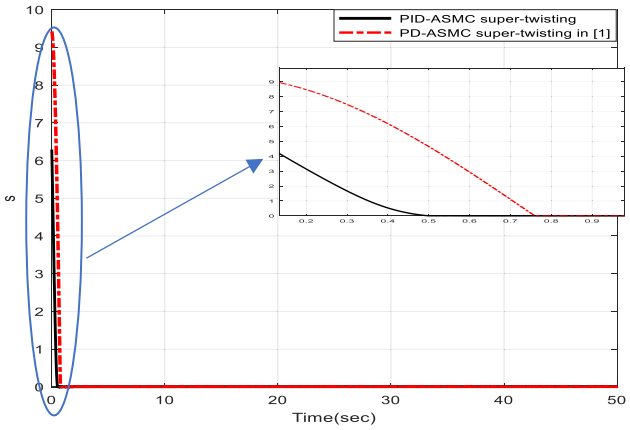

FIGURE 9. Time histories of sliding surface under unknown bound perturbation.

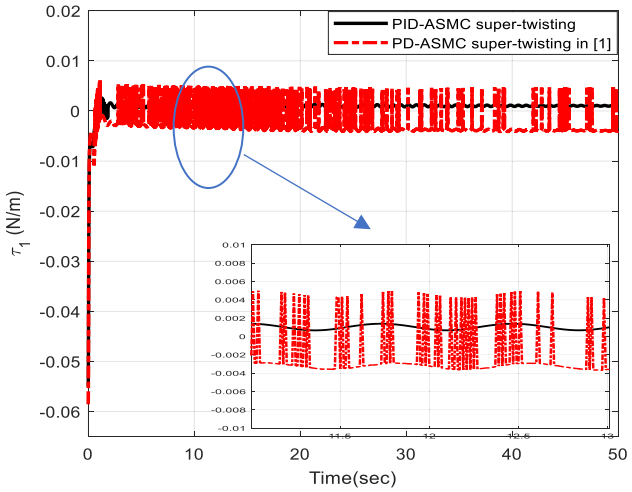

FIGURE 10. Time histories of applied torque using adaptive supper-twisting PID-SMC.

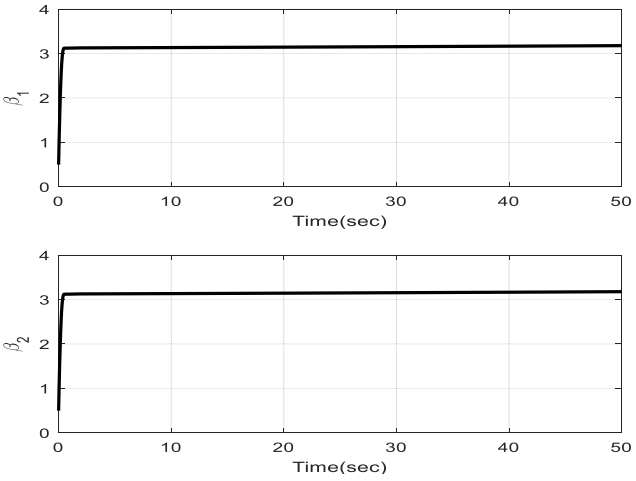

FIGURE 11. Time histories of estimation of upper bound of perturbation.

displayed in Fig.10. From this figure, it can be understood that the chttering phenomenon has been improved in comparison

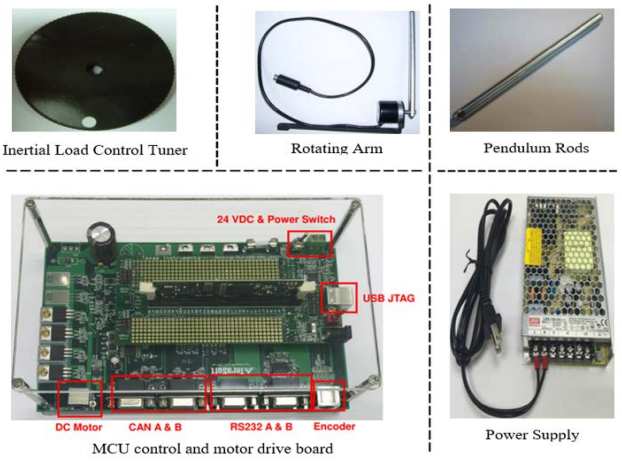

FIGURE 12. Components of EMECS.

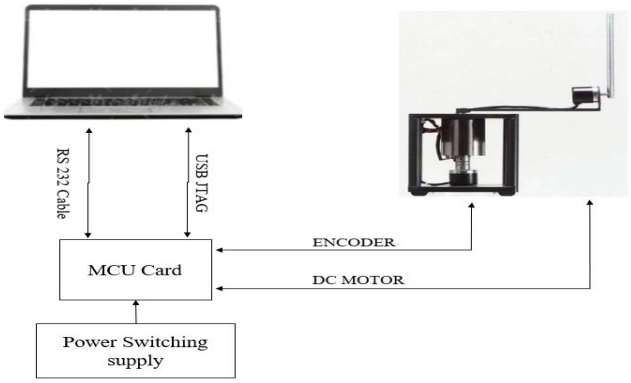

FIGURE 13. Block diagram of the implementing of the proposed method.

with the method of [1]. At last, the adapation laws related to the approximation of upper bound of exterior disturbances are illustrated in Fig.11. Acording to these figures and comparisions, it can be seen that the recommended method based on the adptive super-twisting PID-SMC presents the fast and better transient response in comparison with technique of [1].

B. EXPERIMENTAL RESULTS

In this part, some experimental outcomes are implemented on a real electro-mechanical engineering control system which is developed by the TERASOFT company in Future Technology Research Center (FTRC) in National Yunlin University of Science and Technology. The components of this system are shown in Fig.12. Moreover, this control system has support package in MATLAB as the embedded coder toolbox that supports Texas instruments C2000 Processors. In addition, block diagram of the platform is depicted in Fig.13. The laboratory environment for implementation of the suggested method on real RIP system is exposed in Fig.14.

The applied voltage for motor in the control of RIP system is calculated as the following equation:

$$e = \frac{R_m}{K_t}\left[\tau_1 + \frac{K_t^2}{R_m}\dot{\theta}_1\right], \tag{51}$$

FIGURE 14. Laboratory environment of rotary-inverted-pendulum.

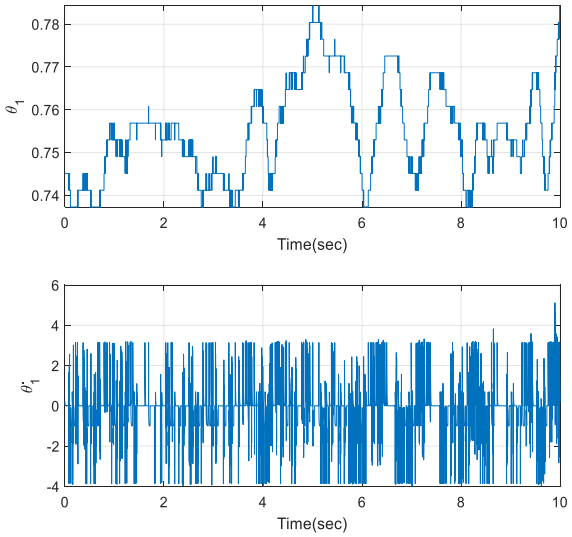

FIGURE 15. Time histories of $\theta_1, \dot{\theta}_1$.

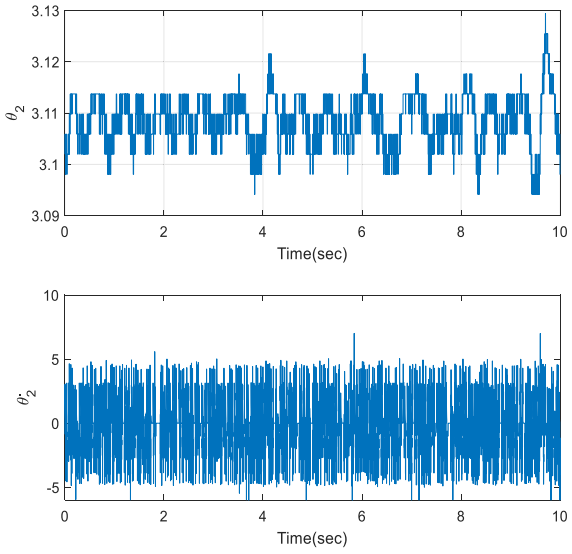

FIGURE 16. Time responses of $\theta_2, \dot{\theta}_2$.

where R_m and K_t are the motor armature resistance and motor torque constants.

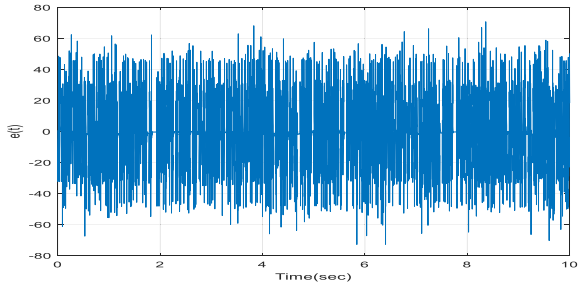

FIGURE 17. Applied voltage for DC Motor.

After implementing the suggested method on the RIP system, the subsequent outcomes are found. Time responses of the position and angular velocities of the arm and pendulum are shown in Fig.15 and Fig.16, individually. It can be seen that the position of arm is stabilized near 0.7 degree which is equal to 0.012 radian. Additionally, the pendulum position is converged to zero (around 3.11 degree). So, the positions of the arm and pendulum are stabilized to a region near the origin. In VI, time trajectory of the applied voltage in DC motor is displayed. Hence, the validation of the suggested method is proved.

VI. CONCLUSION

In this paper, the dynamical model of rotational inverted pendulum system was studied in the form of state-space model. The finite time stability of the rotary inverted pendulum system under known bounded exterior disturbance was accomplished according to the super-twisting PID sliding mode control. Whereas the upper bound of perturbation was assumed to be unknown and the adaptive-tuning control scheme was designed to estimate the unknown bounds. In addition, the Lyapunov stability theory was used to attest the stability control of underactuated rotary inverted pendulum based on the adaptive super-twisting PID sliding mode control technique. As well, simulation results were provided based on the recommended method. The simulation outcomes were compared with another method which was confirmed the proficiency and efficacy of the suggested procedure in comparison with the other method. Furthermore, experimental results on real RIP were provided to demonstrate the efficiency of the planned method.

ACKNOWLEDGMENT

The authors would like to acknowledge Chih-Ming Chang, Department of Technical Expert, Terasoft Company, Taiwan, for his outstanding service, invaluable support and useful suggestions. Data Availability: The data which support the findings of this research are available within the paper.

REFERENCES

[1] N. P. Nguyen, H. Oh, Y. Kim, J. Moon, J. Yang, and W.-H. Chen, "Fuzzy-based super-twisting sliding mode stabilization control for underactuated rotary inverted pendulum systems," *IEEE Access*, vol. 8, pp. 185079–185092, 2020.

[2] Z. Ping, H. Hu, Y. Huang, S. Ge, and J.-G. Lu, "Discrete-time neural network approach for tracking control of spherical inverted pendulum," *IEEE Trans. Syst., Man, Cybern., Syst.*, vol. 50, no. 8, pp. 2989–2995, Aug. 2020.

[3] D. Galan, D. Chaos, L. de la Torre, E. Aranda-Escolastico, and R. Heradio, "Customized online laboratory experiments: A general tool and its application to the Furuta inverted pendulum [Focus on Education]," *IEEE Control Syst.*, vol. 39, no. 5, pp. 75–87, Oct. 2019.

[4] Z. Ben Hazem, M. J. Fotuhi, and Z. Bingul, "A comparative study of the joint neuro-fuzzy friction models for a triple link rotary inverted pendulum," *IEEE Access*, vol. 8, pp. 49066–49078, 2020.

[5] I. M. Mehedi, U. Ansari, A. H. Bajodah, U. M. Al-Saggaf, B. Kada, and M. J. Rawa, "Underactuated rotary inverted pendulum control using robust generalized dynamic inversion," *J. Vib. Control*, vol. 26, nos. 23–24, pp. 2210–2220, 2020.

[6] G. Pujol-Vazquez, L. Acho, S. Mobayen, A. Nápoles, and V. Pérez, "Rotary inverted pendulum with magnetically external perturbations as a source of the pendulum's base navigation commands," *J. Franklin Inst.*, vol. 355, no. 10, pp. 4077–4096, 2018.

[7] P. Dwivedi, S. Pandey, and A. Junghare, "Performance analysis and experimental validation of 2-DOF fractional-order controller for underactuated rotary inverted pendulum," *Arabian J. Sci. Eng.*, vol. 42, no. 12, pp. 5121–5145, Dec. 2017.

[8] I. Yiit, "Model free sliding mode stabilizing control of a real rotary inverted pendulum," *J. Vib. Control*, vol. 23, no. 10, pp. 1645–1662, 2017.

[9] S. H. Zabihifar, A. S. Yushchenko, and H. Navvabi, "Robust control based on adaptive neural network for Rotary inverted pendulum with oscillation compensation," *Neural Comput. Appl.*, vol. 32, pp. 14667–14679, Mar. 2020.

[10] N. P. Nguyen, H. Oh, Y. Kim, and J. Moon, "A nonlinear hybrid controller for swinging-up and stabilizing the rotary inverted pendulum," *Nonlinear Dyn.*, vol. 104, no. 2, pp. 1117–1137, 2021.

[11] M. F. Hamza, H. J. Yap, I. A. Choudhury, A. I. Isa, A. Y. Zimit, and T. Kumbasar, "Current development on using rotary inverted pendulum as a benchmark for testing linear and nonlinear control algorithms," *Mech. Syst. Signal Process.*, vol. 116, pp. 347–369, Feb. 2019.

[12] Y. Wang, T. Wang, X. Yang, and J. Yang, "Decentralized optimal tracking control for large-scale nonlinear systems with tracking error constraints," *Int. J. Adapt. Control Signal Process.*, vol. 35, no. 7, pp. 1388–1403, 2021.

[13] O. Mofid, K. A. Alattas, S. Mobayen, M. T. Vu, and Y. Bouteraa, "Adaptive finite-time command-filtered backstepping sliding mode control for stabilization of a disturbed rotary-inverted-pendulum with experimental validation," *J. Vib. Control*, to be published, doi: 10.1177/10775463211064022.

[14] A. Barkat, M. T. Hamayun, S. Ijaz, S. Akhtar, E. A. Ansari, and I. Ghous, "Model identification and real-time implementation of a linear parameter–varying control scheme on lab-based inverted pendulum system," *Proc. Inst. Mech. Eng., I, J. Syst. Control Eng.*, vol. 235, no. 1, pp. 30–38, 2021.

[15] O. Saleem and K. Mahmood-Ul-Hasan, "Indirect adaptive state-feedback control of rotary inverted pendulum using self-mutating hyperbolic-functions for online cost variation," *IEEE Access*, vol. 8, pp. 91236–91247, 2020.

[16] P. Dwivedi, S. Pandey, and A. S. Junghare, "Stabilization of unstable equilibrium point of rotary inverted pendulum using fractional controller," *J. Franklin Inst.*, vol. 354, no. 17, pp. 7732–7766, Nov. 2017.

[17] T. Horibe and N. Sakamoto, "Optimal swing up and stabilization control for inverted pendulum via stable manifold method," *IEEE Trans. Control Syst. Technol.*, vol. 26, no. 2, pp. 708–715, Mar. 2018.

[18] C.-F. Huang and T.-J. Yeh, "Anti slip balancing control for wheeled inverted pendulum vehicles," *IEEE Trans. Control Syst. Technol.*, vol. 28, no. 3, pp. 1042–1049, May 2020.

[19] Z. Ping, C. Liu, Y. Huang, M. Yu, and J.-G. Lu, "Experimental output regulation of linear motor driven inverted pendulum with friction compensation," *IEEE Trans. Syst., Man, Cybern., Syst.*, vol. 51, no. 6, pp. 3751–3758, Jun. 2021.

[20] S. Liang, Z. Wang, and G. Stepan, "Motion control of a two-wheeled inverted pendulum with uncertain rolling resistance and angle constraint based on slow-fast dynamics," *Nonlinear Dyn.*, vol. 104, no. 3, pp. 2185–2199, May 2021.

[21] O. Saleem and K. Mahmood-ul-Hasan, "Robust stabilisation of rotary inverted pendulum using intelligently optimised nonlinear self-adaptive dual fractional-order PD controllers," *Int. J. Syst. Sci.*, vol. 50, no. 7, pp. 1399–1414, May 2019.

[22] L.-G. Lin and M. Xin, "Nonlinear control of two-wheeled robot based on novel analysis and design of SDRE scheme," *IEEE Trans. Control Syst. Technol.*, vol. 28, no. 3, pp. 1140–1148, May 2020.

[23] C. Liu, Z. Ping, Y. Huang, J.-G. Lu, and H. Wang, "Position control of spherical inverted pendulum via improved discrete-time neural network approach," *Nonlinear Dyn.*, vol. 99, no. 4, pp. 2867–2875, Mar. 2020.

[24] B. Ranjbar, A. Ranjbar Noiey, and B. Rezaie, "Decentralized adaptive terminal sliding mode control design for nonlinear connected system in the presence of external disturbance," *Int. J. Adapt. Control Signal Process.*, vol. 35, no. 10, pp. 2094–2107, Oct. 2021.

[25] S. Mobayen and F. Tchier, "An LMI approach to adaptive robust tracker design for uncertain nonlinear systems with time-delays and input nonlinearities," *Nonlinear Dyn.*, vol. 85, no. 3, pp. 1965–1978, 2016.

[26] R. Rahmani, S. Mobayen, A. Fekih, and J. Ro, "Robust passivity cascade technique-based control using RBFN approximators for the stabilization of a cart inverted pendulum," *Mathematics*, vol. 9, no. 11, p. 1229, Jan. 2021.

[27] O. Saleem, M. Rizwan, and K. Mahmood-ul-Hasan, "Self-tuning state-feedback control of a rotary pendulum system using adjustable degree-of-stability design," *Automatika*, vol. 62, no. 1, pp. 84–97, Jan. 2021.

[28] X. Yang and X. Zheng, "Swing-up and stabilization control design for an underactuated rotary inverted pendulum system: Theory and experiments," *IEEE Trans. Ind. Electron.*, vol. 65, no. 9, pp. 7229–7238, Sep. 2018.

[29] M. Muehlebach and R. D'Andrea, "Nonlinear analysis and control of a reaction-wheel-based 3-D inverted pendulum," *IEEE Trans. Control Syst. Technol.*, vol. 25, no. 1, pp. 235–246, Jan. 2017.

[30] A. Mustafa, N. K. Dhar, and N. K. Verma, "Event-triggered sliding mode control for trajectory tracking of nonlinear systems," *IEEE/CAA J. Automatica Sinica*, vol. 7, no. 1, pp. 307–314, Jan. 2020.

[31] M. Mohamed, X. Yan, Z. Mao, and B. Jiang, "Adaptive observer design for nonlinear interconnected systems by the application of LaSalle's theorem," *Int. J. Adapt. Control Signal Process.*, vol. 34, no. 11, pp. 1559–1571, Nov. 2020.

[32] Z. B. Hazem, M. J. Fotuhi, and Z. Bingül, "Development of a fuzzy-LQR and fuzzy-LQG stability control for a double link rotary inverted pendulum," *J. Franklin Inst.*, vol. 357, no. 15, pp. 10529–10556, Oct. 2020.

[33] T. F. Tang, S. H. Chong, and K. K. Pang, "Stabilisation of a rotary inverted pendulum system with double-PID and LQR control: Experimental verification," *Int. J. Automat. Control*, vol. 14, no. 1, pp. 18–33, 2020.

[34] I. Chawla and A. Singla, "Real-time control of a rotary inverted pendulum using robust LQR-based ANFIS controller," *Int. J. Nonlinear Sci. Numer. Simul.*, vol. 19, nos. 3–4, pp. 379–389, Jun. 2018.

[35] I. Jmel, H. Dimassi, S. Hadj-Said, and F. M'Sahli, "An adaptive sliding mode observer for inverted pendulum under mass variation and disturbances with experimental validation," *ISA Trans.*, vol. 102, pp. 264–279, Jul. 2020.

[36] P. N. Dao and Y.-C. Liu, "Adaptive reinforcement learning strategy with sliding mode control for unknown and disturbed wheeled inverted pendulum," *Int. J. Control, Automat. Syst.*, vol. 19, pp. 1139–1150, Dec. 2020.

[37] H. Ouyang, J. Wang, G. Zhang, L. Mei, and X. Deng, "Novel adaptive hierarchical sliding mode control for trajectory tracking and load sway rejection in double-pendulum overhead cranes," *IEEE Access*, vol. 7, pp. 10353–10361, 2019.

[38] C. Xu, D. Tong, Q. Chen, W. Zhou, and P. Shi, "Exponential stability of Markovian jumping systems via adaptive sliding mode control," *IEEE Trans. Syst., Man, Cybern., Syst.*, vol. 51, no. 2, pp. 954–964, Feb. 2021.

[39] S. Ahmed, H. Wang, and Y. Tian, "Adaptive high-order terminal sliding mode control based on time delay estimation for the robotic manipulators with backlash hysteresis," *IEEE Trans. Syst., Man, Cybern., Syst.*, vol. 51, no. 2, pp. 1128–1137, Feb. 2021.

[40] H. Habibi, I. Howard, S. Simani, and A. Fekih, "Decoupling adaptive sliding mode observer design for wind turbines subject to simultaneous faults in sensors and actuators," *IEEE/CAA J. Automatica Sinica*, vol. 8, no. 4, pp. 837–847, Apr. 2021.

[41] S. B. Prusty, S. Seshagiri, U. C. Pati, and K. K. Mahapatra, "Sliding mode control of coupled tank systems using conditional integrators," *IEEE/CAA J. Automatica Sinica*, vol. 7, no. 1, pp. 118–125, Jan. 2020.

[42] A. T. Azar and F. E. Serrano, "Adaptive sliding mode control of the Furuta pendulum," in *Advances and Applications in Sliding Mode Control systems* (Studies in Computational Intelligence), vol. 576, A. Azar and Q. Zhu, Eds. Cham, Switzerland: Springer, 2015, doi: 10.1007/978-3-319-11173-5_1.

[43] X. Liu, M. Zhang, J. Chen, and B. Yin, "Trajectory tracking with quaternion-based attitude representation for autonomous underwater vehicle based on terminal sliding mode control," *Appl. Ocean Res.*, vol. 104, Nov. 2020, Art. no. 102342.

FAYEZ F. M. EL-SOUSY (Member, IEEE) received the B.Sc. degree in electrical engineering from Menoufia University, Egypt, in 1988, and the M.Sc. and Ph.D. degrees in electrical engineering from Cairo University, Giza, Egypt, in 1994 and 2000, respectively. From 1988 to 2019, he was with the Department of Power Electronics and Energy Conversion, Electronics Research Institute, Giza, where he was a Full Professor. From August 1995 to June 2000, he was a Lecturer with the Department of Electrical Engineering, October Six University, Giza, where he was an Assistant Professor with the Department of Electrical Engineering, from August 2000 to June 2003. From April 2004 to February 2007, he was a Postdoctoral Visiting Researcher at the Graduate School of Information Science and Electrical Engineering, Kyushu University, Fukuoka, Japan. From 2007 to 2010, he was an Associate Professor and the Chair of the Department of Electrical Engineering, College of Engineering, King Saud University, Riyadh, Saudi Arabia. From 2010 to 2014, he was an Associate Professor and the Chair of the Department of Electrical Engineering, College of Engineering, Salman bin Abdulaziz University, Al-Kharj, Saudi Arabia. Since 2014, he has been a Full Professor and the Vice Chair with the Department of Electrical Engineering, College of Engineering, Prince Sattam Bin Abdulaziz University, Saudi Arabia. His research interests include modeling and control of motor drives, motion-control systems, wind energy systems, digital signal processing-based computer control systems, computational intelligent of power electronics, electric drives and power systems, intelligent control theories including fuzzy logic, neural networks, and wavelets, nonlinear control and optimal control, and robust control. His current research interests include intelligent control of smart grid and DC micro grid.

KHALID A. ALATTAS (Member, IEEE) received the B.Sc. degree in computer science from King Abdulaziz University, Saudi Arabia, the M.Sc. degree in telecommunication networks from New York University, NY, USA, and the M.Sc. and Ph.D. degrees in computer science from the University of Louisiana at Lafayette, USA. He is currently an Assistant Professor with the College of Computer Science and Engineering, University of Jeddah, Saudi Arabia. His research interests include networks, machine learning, and data analytics. He serves as a reviewer for many international journals.

OMID MOFID received the B.Sc. degree in mathematical sciences and applications from the University of Tafresh, in 2015, and the M.Sc. degree in control engineering from the University of Zanjan, in 2017. He is currently working at the Future Technology Research Center, National Yunlin University of Science and Technology, Taiwan, as a Researcher. His major research interests include quad-rotor UAV, rotary-inverted-pendulum, chaotic systems and robot manipulator based on the adaptive, and sliding mode control.

SALEH MOBAYEN (Senior Member, IEEE) was born in Khoy, Iran, in 1984. He received the B.Sc. and M.Sc. degrees in electrical engineering, area: control engineering from the University of Tabriz, Tabriz, Iran, in 2007 and 2009, respectively, and the Ph.D. degree in electrical engineering, area: control engineering from Tarbiat Modares University, Tehran, Iran, in January 2013. From January 2013 to December 2018, he was as an Assistant Professor and a Faculty Member with the Department of Electrical Engineering, University of Zanjan, Zanjan, Iran. Since December 2018, he has been an Associate Professor of control engineering at the Department of Electrical Engineering, University of Zanjan. From July 2019 to September 2019, he was a Visiting Professor at the University of the West of England (UWE), Bristol, U.K., with financial support from the Engineering Modeling and Simulation Research Group, Department of Engineering Design and Mathematics. Since 2020, he has been an Associate Professor at the National Yunlin University of Science and Technology (YunTech), Taiwan, and collaborated with the Future Technology Research Center (FTRC). He has published several papers in the national and international journals. His research interests include control theory, sliding mode control, robust tracking, non-holonomic robots, and chaotic systems. He is a member of the IEEE Control Systems Society and serves as a member for program committee of several international conferences. He is an associate editor of several international scientific journals and has acted as a symposium/the track co-chair in numerous IEEE flagship conferences. He has been a world's top 2% scientist from Stanford University, since 2019, and has been ranked among 1% top scientists in the world in the broad field of electronics and electrical engineering. He is also recognized in the list of Top Electronics and Electrical Engineering Scientists in Iran.

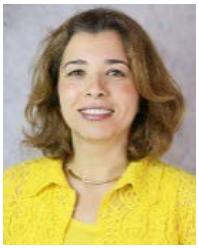

AFEF FEKIH (Senior Member, IEEE) received the B.S., M.S., and Ph.D. degrees in electrical engineering from the National Engineering School of Tunis, Tunisia, in 1995, 1998, and 2002, respectively. She is currently a Full Professor with the Department of Electrical and Computer Engineering and the Chevron/BORSF Professor in engineering at the University of Louisiana at Lafayette. Her research interests include control theory and applications, including nonlinear and robust control, optimal control, fault tolerant control with applications to power systems, wind turbines, unmanned vehicles, and automotive engines. She is a member of the IEEE Control Systems Society and the IEEE Women in Control Society.